PHYSICAL REVIEW E **74**, 050701(R) (2006)

Anticonical anchoring and surface transitions in a nematic liquid crystal

L. Faget,[1] S. Lamarque-Forget,[1] Ph. Martinot-Lagarde,[1,2] P. Auroy,[3] and I. Dozov[1,*]
[1]*Nemoptic, Parc du Mérantais, 1 rue Guynemer, F-78114 Magny-les-Hameaux, France*
[2]*Laboratoire de Physique des Solides, Université Paris-Sud, Bâtiment 510, Orsay, France*
[3]*Institut Curie, UMR 168 du CNRS, 11 rue Pierre et Marie Curie, F-75231 Paris Cedex 05, France*
(Received 3 June 2006; published 30 November 2006)

Recent works reported planar and conical azimuthally degenerated nematic anchorings. Here we predict an additional "anticonical" degenerated anchoring. Its energy presents two minima, parallel and perpendicular to the substrate plane, separated by a conical energy barrier. We realize this bistable anchoring on a grafted polymer brush and we observe temperature-driven transitions between the conical, planar, and anticonical degenerated anchorings. Under electric field we break the anticonical anchoring and switch between its bistable states.

DOI: 10.1103/PhysRevE.74.050701 PACS number(s): 61.30.Gd, 61.30.Hn, 68.08.−p

The alignment and the anchoring of nematic liquid crystals (NLCs) on the boundary surfaces is important for both fundamental research and applications. In the bulk, the order parameter tensor $\mathbf{Q}=(3/2)\mathrm{S}(\mathbf{nn}-\mathbf{I}/3)$ orientation, defined by the director $\mathbf{n}$, is arbitrary. Surface interactions broke the rotational invariance of $\mathbf{Q}$ and define some "easy" axes $\mathbf{n}_e$ for the surface director $\mathbf{n}_s$ orientation. For the most common monostable anchorings $\mathbf{n}_e$ is unique and any deviation $\delta\mathbf{n}_s=\mathbf{n}_s-\mathbf{n}_e$ costs some anchoring energy $W(\delta\mathbf{n}_s)$. In a first approximation $W(\delta\mathbf{n}_s)$ can be presented as a sum of two independent zenithal and azimuthal Rapini-Papoular (RP) $\cos^2$ terms [1],

$$W(\theta_s,\varphi_s)=-\frac{1}{2}A_{zen}\cos^2(\theta_s-\theta_e)-\frac{1}{2}A_{az}\cos^2(\varphi_s-\varphi_e)$$

where θ_s, φ_s are the spherical coordinates of $\mathbf{n}_s$ and A_{zen}, A_{az} are the anchoring strength coefficients.

Bistable or multistable anchorings, with several distinct easy axes, have been reported on cleaved crystals [2], evaporated SiO films [3], and nanostructured [4,5] polymers. Continuously degenerated anchorings, with energy minimized on an "easy surface" instead of on a manifold of distinct easy axes, could also exist. By symmetry reasons, zenithal degeneration cannot be expected; the surface normal $\mathbf{N}$ is a particular direction, due to the intrinsic asymmetry of the nematic-substrate interface and the strong order gradients $\nabla\mathbf{Q}$ along $\mathbf{N}$. On the contrary, on isotropic surfaces all the azimuthal directions are equivalent and A_{az} should vanish. On solid substrates the azimuthal degeneration is often hindered by the anchoring memory [6–8]. However, memory-free degenerated alignments on polymer surfaces were recently reported, either planar (Pl), with "easy plane" defined by $\theta_s=\pi/2$ [9] or conical (Co), with "easy cone" $\theta_s=\theta_c<\pi/2$ [10].

The simple RP approximation is inadequate for multistable and degenerated anchorings. Higher order terms in $\cos\pi$ (and eventually zenithal-azimuthal coupling terms [3]) are needed in this case, e.g., a large $\cos^4\theta$ term is required [10] to explain the conical anchoring. Recently, Fournier and Galatola [11] described degenerated anchorings by introducing $\mathbf{Q}^4$ terms in the surface energy expansion, leading to large non-RP terms in $W(\theta_s,\varphi_s)$. Large, high-order terms have been experimentally detected close to anchoring transitions, driven by the temperature or by the surface treatment, e.g., the monostable-bistable transition on SiO [12] or the homeotropic-tilted transition on rubbed polyimide [13].

Here we discuss the most general symmetry-allowed form of the azimuthally degenerated anchoring energy. Including large non-RP terms, we predict an anticonical anchoring with two energy minima, planar degenerated and homeotropic, separated by a conical energy barrier. We realize this bistable anchoring on a grafted polymer and we observe temperature-driven transitions between the three degenerated anchoring states—conical, planar, and anticonical. Under moderate electric field we break the anticonical anchoring and we switch between the bistable states.

For azimuthally degenerated anchorings the anchoring energy $W=W(\theta_s)$ is φ_s independent. The symmetry of the surface (revolution) and of the nematic (inversion) imposes $W(\theta_s)=W(-\theta_s)=W(\pi\pm\theta_s)$. The most general form of $W(\theta_s)$ is given by the Fourier expansion

$$W(\theta_S)=\frac{1}{2}\alpha\cos(2\theta_S)+\frac{1}{4}\beta\cos(4\theta_s)+\frac{1}{6}\gamma\cos(6\theta_s)+\frac{1}{8}\delta\cos(8\theta_s)+\ldots, \quad (1)$$

where α is the RP term and $\beta,\gamma,\ldots$ are higher order contributions. Keeping only α and minimizing, we obtain either Pl degeneration ($\alpha>0$) or monostable homeotropic (Ho) state ($\alpha<0$). To describe the Co state we need higher order terms (for simplicity we keep here only β, see the discussion below about $\gamma,\delta,\ldots$).

The "phase" diagram of the anchoring, obtained by minimization of $W(\theta_s)$ is presented in Fig. 1(a). For $|\alpha|>2|\beta|$, the anchoring is planar ($\alpha>0$) or homeotropic ($\alpha<0$). For $2\beta>|\alpha|$ the anchoring is conical, with energy maxima for $\theta_s=0$, $\pi/2$ and a minimum on the easy cone $\theta_c=\frac{1}{2}\arccos(-\alpha/2\beta)$. The Pl and Co degenerated anchorings

*Corresponding author. Email address: i.dozov@nemoptic.com

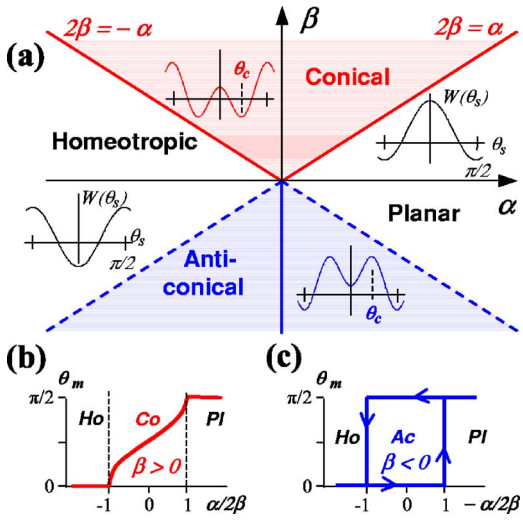

FIG. 1. (Color online) Phase diagram for azimuthally degenerated anchorings. (a) Anchoring states as a function of the anchoring strength parameters α and β. The insets show schematically the energy function $W(\theta_s)$ for the corresponding region. (b) Consecutive second-order planar-conical and conical-homeotropic anchoring transitions. (c) First-order planar-homeotropic transition with hysteresis loop surrounding the anticonical anchoring domain.

have been already reported experimentally [9,10]. For $2\beta < -|\alpha|$, however, a qualitatively different anchoring is obtained: $W(\theta)$ has two minima for $\theta_s=0,\pi/2$ and is maximized on the "difficult cone" $\theta_c=\frac{1}{2}\arccos(-\alpha/2\beta)$. This *anticonical* (Ac) anchoring is bistable; the two minima (homeotropic and planar) are separated by the difficult cone energy barrier.

By analogy with the phase transitions [14], we expect anchoring transitions when α and β vary. Plotting for $\beta>0$ the absolute energy minimum θ_m, we obtain two second-order (continuous) transitions [Fig. 1(b)], Pl-Co and Co-Ho, already reported experimentally [15]. Due to the high-order terms in Eq. (1), the anchoring strength remains finite at these transitions. Only at $\alpha=\beta=0$ we obtain $W(\theta_s)\equiv 0$ and first-order Ho-Pl transition, never reported and quite improbable (there are no symmetry arguments to justify $\alpha=\beta=\ldots=0$).

For $\beta<0$, the absolute energy minimum jumps from $\theta_m=\pi/2$ to $\theta_m=0$ at the $\alpha=0$ line, giving a first-order (discontinuous) Pl-Ho transition. The Ac anchoring is then an analog of the phase coexistence close to a first-order phase transition [Fig. 1(c)]; the Ho state is "superheated" up to $\alpha=-2\beta$, the Pl state is "supercooled" down to $\alpha=2\beta$. Once more, the anchoring barrier height remains finite at the transition.

In the experiments we use a grafted polystyrene (PS) surface, reported [10] to give conical anchoring with *n*-pentyl-cyanobyphenyl (5CB). To modify the anchoring (and hence α and β) to anticonical, we vary the nematic compound and the PS grafting density. The results reported here are obtained with 7CB on 10-nm-thick PS layer.

Monodisperse polystyrene, trichlorosilane ($SiCl_3$) terminated on one side, was synthesized and grafted [10,16] on silicium wafers (for ellipsometric measurements) and on indium-tin oxide (ITO) covered glass plates (for the anchoring studies). The average dry thickness h_{dry} of the layer is adjusted in the range 25–150 Å by grafting density variation. The active $SiCl_3$-terminated polymer is mixed in controlled proportion R_{act} with inert PS. During the grafting the two species are in competition for adsorption and/or chemical reaction with the surface. Toluene washing after the grafting removes the inert polymer, leaving a film with thickness h_{dry} controlled by R_{act}. The ellipsometric measurements of h_{dry} on the wafer and on the ITO-covered plates (with lower precision) are in reasonable agreement, showing good reproducibility of the grafting. The results presented here are obtained with $h_{dry}=102\pm5$ Å and average distance between the grafting points $D=21.2\pm0.4$ Å. The ratio $h_{dry}/D\cong 5$ shows that the grafted layer is in a brush regime. The grafted brush is stable, without anchoring properties variation, after several months in contact with the NLC.

Qualitatively, we identify the anchoring state by observation of the texture defects. The PS-grafted substrate is mounted in a cell holder [9], enabling variation of the cell gap $d(1-100\ \mu\text{m})$, to twist the cell at an arbitrary angle and to change at will the counterplate (typically ITO-covered spherical lens with strong planar or homeotropic anchoring). Quantitative results are obtained by electro-optic measurements, using thin ($d\cong 1.5\ \mu$m) sealed cells with one PS-grafted substrate and a planar anchoring counterplate (both of them ITO covered). The thin cell ensures fast bulk relaxation (<10 ms). Our experimental setup [17,18], mounted on a polarizing microscope, measures the optical retardation $L(U)$ as a function of the applied voltage U. The field is applied in 100 kHz ac bursts to avoid artifacts related to electrochemical degradation, ionic transport, and polar coupling. During the burst, U varies continuously from zero up to several volts and then back to zero, giving in one burst the two-way electro-optical curve, detecting eventual hysteresis. To smooth the data, 10–20 acquisitions are accumulated. At low voltage, below the Fréedericksz [19] threshold U_F, we measure [10,17] the conic pretilt $\psi_c=\pi/2-\theta_c$. At stronger fields, we detect the anchoring breaking threshold [10,20,21], continuous or discontinuous, giving the anchoring strength $d^2W/d\theta_s^2=2\alpha+4\beta+\ldots$.

Cooling down from the isotropic phase, below the nematic-isotropic transition ($T_{NI}=42.0\ ^\circ$C) we observe a conical anchoring, with coexisting twin domains [Fig. 2(a)], separated by mobile surface walls. From the ψ_c measurement we obtain $\alpha/\beta=2\cos(2\psi_c)$. At increasing U, $\mathbf{n}_s$ rotates under the dielectric torque $\Gamma_{diel}\cong\pi K_{33}\theta_s U/(dU_F)$ (here $K_{33}=K_{11}$ and $U\gg U_F$ are supposed) and the birefringence decreases. At a threshold voltage $U_\perp\cong dU_F(2\alpha+4\beta+\ldots)/(\pi K_{33})$ we observe [Fig. 2(d)] a second-order anchoring breaking [10,20] on the PS substrate: $\mathbf{n}_s$ rotates to the maximum of $W(\theta_s)$ at $\theta_s=0$, and the anchoring torque $\Gamma_{anc}=\partial W(\theta_s)/\partial\theta_s$ vanishes. Above $U_\perp$, $\theta_s\equiv 0$ and all the birefringence comes from the thin distorted region close to the strongly anchored counterplate. From $U_\perp$ and ψ_c we obtain the α,β values, plotted in Fig. 3(b).

Upon decreasing the temperature, ψ_c decreases [Fig. 3(a)] and at 30.5 °C we observe the Co-Pl transition: the conical twin domains disappear [Fig. 2(b)] when the $W(\theta_s=\pi/2)$ maximum transforms into a minimum. The sharp threshold

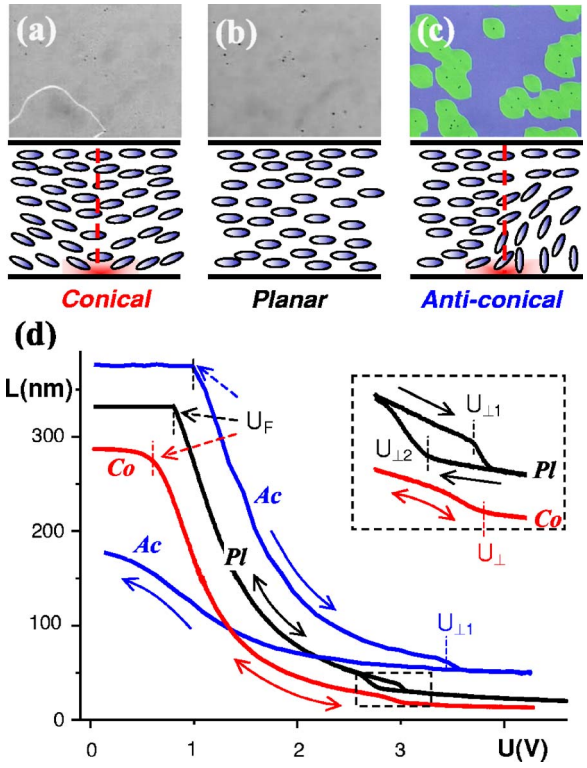

FIG. 2. (Color online) Experimentally observed degenerated anchorings. Photographs (top) and schema of the textures (middle). (a) Conical state at $T=32.5\ ^\circ\mathrm{C}$ identified by the twin domains. (b) Planar state at $T=24.5\ ^\circ\mathrm{C}$, evidenced by the lack of defects. (c) Anticonical state at $T=7.5\ ^\circ\mathrm{C}$ with coexisting planar ($\theta_s=\pi/2$) and hybrid ($\theta_s=0$) domains. (d) Electro-optical results. For clear separation the Pl and the Ac curves have been shifted upward by 10 and 30 nm, respectively. The inset zooms on the anchoring breaking regions.

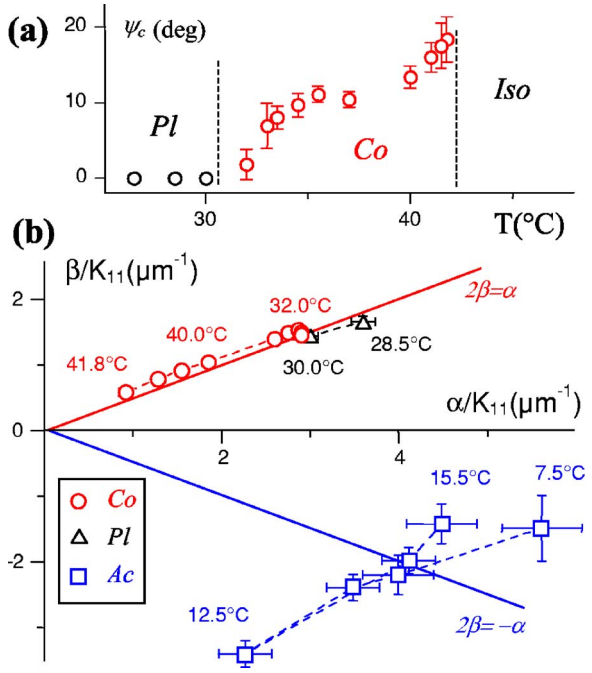

FIG. 3. (Color online) Temperature variation of the anchoring state. (a) Conical pretilt angle $\psi_c=\pi/2-\theta_c$. (b) Path of the state in the α,β phase space. The anchoring strength coefficients are renormalized with the splay elastic constant K_{11}. The thick lines delimit the three anchoring regions in Fig. 1. The symbols show the anchoring state directly observed in the experiment.

at $U=U_F$ confirms $\psi_c=0$. Above $T=25\ ^\circ\mathrm{C}$ the anchoring breaking threshold $U_\perp$ still gives us the anchoring strength $2\alpha+4\beta+\ldots$, but due to $\psi_c=0$ we cannot obtain separately α and β. Below $25\ ^\circ\mathrm{C}$ the electro-optical curve [Fig. 2(d)] shows a first-order anchoring breaking [20] with a hysteresis loop, limited by the thresholds $U_{\perp 1}$ and $U_{\perp 2}$. This behavior, already described for tilted monostable anchorings, is expected close to the Pl-Ac transition: the flat $W(\theta_s=0)$ maximum transforms under field into a local minimum of the total energy. At the thresholds $U_{\perp 1}$ and $U_{\perp 2}$ the surface director jumps back and forth over the total-energy barrier, resulting in finite jumps of the birefringence ΔL_1 and ΔL_2. In principle, from $U_{\perp 1}$, $U_{\perp 2}$, ΔL_1, and ΔL_2 we can obtain the first four coefficients in Eq. (1). However, the precision of the α,β values obtained in this way is not satisfactory and these data are not presented in Fig. 3(b) (see the discussion below about $\gamma,\delta\neq 0$).

Cooling again, the hysteresis loop enlarges, and at $T=16.4\ ^\circ\mathrm{C}$ we obtain $U_{\perp 2}=0$: the anticonical state is reached and the metastable homeotropic minimum persists without field. Under field the hybrid domains of Fig. 2(c) (homeotropic on the Ac-plate) are favored and grow. Without field, they transit back to the planar state by slow propagation (a few seconds at $16\ ^\circ\mathrm{C}$, several hours at $6\ ^\circ\mathrm{C}$) of the Ac-anchoring characteristic defects [Fig. 2(c)]. The initial and final birefringence values at $U=0$ differ by a factor ~ 2, confirming the transition from planar to hybrid texture. The α,β path in Fig. 3(b), calculated from $U_{\perp 1}$ and ΔL_1, is noisy and displaced toward the planar anchoring region, due again to the neglected $\gamma,\delta,\ldots$ terms.

Qualitatively, our observations agree with the simple phase diagram on Fig. 1: the degenerated Co, Pl, and Ac anchorings are obtained when β varies from strongly positive to strongly negative values. Numerical simulation of the electro-optical curves, keeping the first four terms in Eq. (1), indicates non-negligible γ,δ values, e.g., $\beta/\alpha=-0.26\pm 0.09$, $\gamma/\alpha=0.05\pm 0.03$, $\delta/\alpha=0\pm 0.05$ at $T=17.5\ ^\circ\mathrm{C}$. The two-dimensional (2D) diagrams on Figs. 1(a) and 3(b) are then projections on the α,β-plane of a more complex four-dimensional (4D) phase diagram containing additional, more complicated degenerated states, e.g., with two distinct easy cones separated by an energy barrier.

The observed large values of $\beta,\gamma,\ldots$ require more discussion. To describe all the anchoring states and transitions in the same formalism, we use in Eq. (1) a Fourier expansion, instead of the usual Landau power series. There is no small parameter and the convergence relies only on the expected [22] fast decrease of the high-order coefficients. However, the anchoring transitions and the anchoring breaking thresholds are very sensitive to $d^2W/d\theta_s^2$ and hence, to the high-order coefficients.

The physical origin of the observed large $\beta,\gamma,\ldots$ is not yet clear. Ordoelectricity [23], arising from the strong order gradient across the swollen PS, could explain large positive

β-values [10] but cannot generate negative β, or higher terms. Surface reorganization under torque could also result in large non-RP terms. Some of our observations disagree with the usual description of the anchoring as a simple elastic response of the director to the applied torque Γ. In the planar state, for example, as a function of the field variation rate, we observe either a first- or a second-order anchoring breaking, suggesting a reorganization of the polymer-nematic interface and fast (<10 ms) relaxation to a new equilibrium. $W(\theta_s)$ becomes then an implicit function of $\Gamma=\Gamma(\theta_s)$, with torque-dependent coefficients. In our simple model, describing only equilibrium systems, this leads to apparent large high-order coefficients.

The anticonical anchoring is promising for applications. Unlike other bistable surfaces [4,24,25], the Ac anchoring is realized on isotropic and uniform substrates, without microstructuring. The bistable states, homeotropic and planar, are optically the most distinct possible, ensuring a good contrast. The high energy barrier between them provides good bistability but with low switching threshold, ~ 2 V/μm, compared to >6 V/μm for other weak anchoring [4,21,24,25] surfaces. Bistable devices, using one or two Ac surfaces, switching by polar coupling [16,26–28] or by dual-frequency driving [29], will be reported in a separate paper.

In conclusion, we show that large non-Rapini–Papoular terms lead to a rich anchoring transition behavior on azimuthally degenerated surfaces. The predicted bistable anticonical anchoring and its transitions are observed experimentally. The large non-RP coefficients could be attributed to a torque-induced reorganization of the polymer chains swollen by the ordered NLC. Understanding of the order transitions in the thin, 2D-like interface could lead to the development of different surface bistable nematic devices.

We thank Dr. S. Joly and Dr. D.-N. Stoenescu for helpful discussions and for a critical reading of the manuscript. The work by L.F. was supported by a CIFRE grant from the ANRT, France.

[1] A. Rapini and M. Papoular, J. Phys. (Paris), Colloq. **30**, 54 (1969).
[2] J. Bechhoefer, B. Jerome, and P. Pieranski, Phys. Rev. A **41**, 3187 (1990).
[3] M. Monkade, M. Boix, and G. Durand, Europhys. Lett. **5**, 697 (1988).
[4] G. P. Bryan-Brown, C. V. Brown, I. C. Sage, and V. C. Hui, Nature (London) **392**, 365 (1998).
[5] J.-H. Kim M. Yoneya, and H. Yokoyama, Nature (London) **420**, 159 (2002).
[6] B. Jerome, Rep. Prog. Phys. **54**, 391 (1991).
[7] J. Cheng and G. D. Boyd, Appl. Phys. Lett. **35**, 444 (1979).
[8] R. Barberi *et al.*, Eur. Phys. J. B **6**, 83 (1998).
[9] I. Dozov *et al.*, Appl. Phys. Lett. **77**, 4124 (2000).
[10] O. O. Ramdane *et al.*, Phys. Rev. Lett. **84**, 3871 (2000).
[11] J.-B. Fournier and P. Galatola, Europhys. Lett. **72**, 403 (2005).
[12] M. Nobili and G. Durand, Phys. Rev. A **46**, R6174 (1992); Europhys. Lett. **25**, 527 (1994).
[13] G. Carbone and C. Rosenblatt, Phys. Rev. Lett. **94**, 057802 (2005).
[14] L. D. Landau and E. M. Lifshitz, *Statistical Physics Part 1*, 3rd ed., Course of Theoretical Physics Vol. 5 (Pergamon Press, New York, 1994).
[15] J. S. Patel and H. Yokoyama, Nature (London) **362**, 525 (1993).
[16] O. Ou Ramdane, P. Auroy, and P. Silberzan, Phys. Rev. Lett. **80**, 5141 (1998).
[17] S. Lamarque-Forget, P. Martinot-Lagarde, and I. Dozov, Jpn. J. Appl. Phys., Part 2 **40**, L349 (2001).
[18] S. Lamarque-Forget *et al.*, Adv. Mater. (Weinheim, Ger.) **12**, 1267 (2000).
[19] V. Fréedericksz and V. Zolina, Trans. Faraday Soc. **29**, 919 (1933).
[20] I. Dozov and Ph. Martinot-Lagarde, Phys. Rev. E **58**, 7442 (1998).
[21] I. Dozov, M. Nobili, and G. Durand, , Appl. Phys. Lett. **70**, 1179 (1997).
[22] Fast convergence of the series (1) is expected because the $\cos(2n\theta_s)$ terms derive from the $\mathbf{Q}^n$, terms in the rapidly convergent Landau-de Gennes expansion of the surface free energy.
[23] G. Barbero, I. Dozov, J. F. Palierne, and G. Durand, Phys. Rev. Lett. **56**, 2056 (1986).
[24] R. Barberi, M. Giocondo, Ph. Martinot-Lagarde, and G. Durand, J. Appl. Phys. **62**, 3270 (1993).
[25] R. Barberi, M. Giocondo, J. Li, R. Bartolino, I. Dozov, and G. Durand, Appl. Phys. Lett. **71**, 3495 (1997).
[26] R. B. Meyer, Phys. Rev. Lett. **22**, 918 (1969).
[27] O. D. Lavrentovich *et al.*, Sov. Phys. JETP **72**, 431 (1991).
[28] S. Forget, I. Dozov, and Ph. Martinot-Lagarde, Mol. Cryst. Liq. Cryst. Sci. Technol., Sect. A **329**, 605 (1999).
[29] C. R. Stein, Appl. Phys. Lett. **19**, 343 (1971).